ANALYSIS OF APERTURE ANTENNAS ABOVE LOSSY HALF-SPACE

B. A. Arand, M. Hakkak, and K. Forooraghi

Department of Electrical Engineering
Tarbiat Modarres University
Tehran, Iran

J. R. Mohassel

Department of Electrical Engineering
University of Tehran
Tehran, Iran

Abstract—This paper studies the radiation properties of aperture antennas above imperfect ground using Discrete Complex Image Method (DCIM). The present method is simple and has high accuracy. In this approach, based on linear approximating a function to an exponential series, equivalent complex images have been obtained. Number, intensity and location of images are obtained using Generalized Pencil Of Function (GPOF) technique. We assume current distribution over the aperture be combination of electric and magnetic currents in vertical and horizontal direction. The obtained results are comparable with analytical computation in limited cases. In spite of Sommerfeld integral based methods, this method is simple with lower computational time.

1. INTRODUCTION

Aperture antennas are frequently used in radar and communications. Considering the special application of this kind of antennas researchers have performed different studies and published the achieved results. These antennas are frequently used because of their unique characteristics, such as high gain and wide bandwidth. These important features, distinguish them from others and have provided special applications in terrestrial radio links, satellite communication and radar. As most of these antennas are located above the real ground, so they are considerably effected by it. Up to now, the ground has been considered as a perfect electric conductor so the relevant effects can be easily calculated. But, the effect of the real ground which is a lossy conductor has not been thoroughly studied yet. Therefore, in our investigations, we were seeking the development of a new method to model the ground's effect. Finally, Discrete Complex Image Method (DCIM) was selected as a suitable approach for analyzing the subject. Different approximate methods have been applied for analyzing the short dipole antennas; pointing out some limitations and deficiencies. In previous articles [1, 2], we have mentioned that the new offered method has almost an exact solution for a current element.

This method is applied for wire antennas with considerable length. It was clarified that this method has also an acceptable accuracy [3, 4]. In this paper we extend this approach to two dimensional structures and hereafter develop a new method to analyze the aperture antennas. In addition, our aim is to introduce the simplicity and applicability in
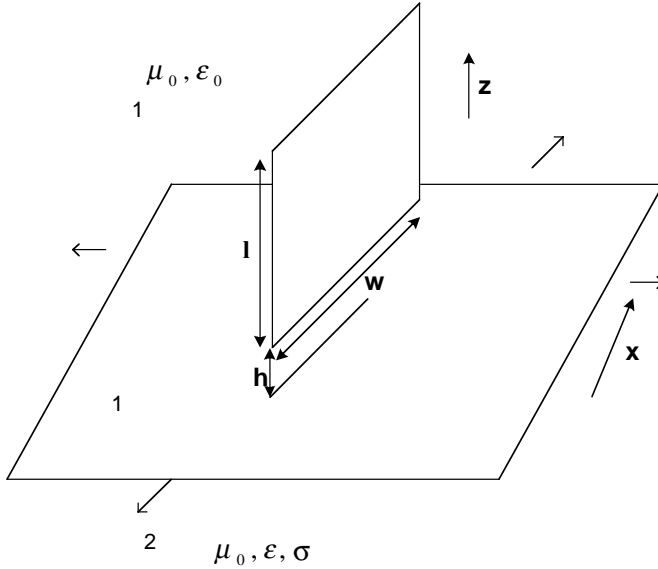
Figure 1. Sketch of aperture antenna above real ground.

pattern calculation above a lossy ground including variations in ground parameters.

2. APERTURE ABOVE GROUND SURFACE

Fig. 1 shows the sketch of aperture antenna above an infinite ground plane. The antenna has dimensions $l \times w$ and located at a height h above the ground surface. Region (2) ($z < 0$) is assumed to be lossy with parameters E_r and σ.

The aperture is located in x-z plane and has the general current distribution, $\vec{J}$. It is assumed that the current is of electric or magnetic type and in an arbitrary direction.

Using the results of short dipole current element and superposition principle, the radiation field of aperture distribution can be written as follows [5]:

$$\vec{E} = C \int_{\frac{-l}{2}}^{\frac{l}{2}} \int_{\frac{-w}{2}}^{\frac{w}{2}} (G)\vec{J}dz'dx' \tag{1}$$

where G is the associated Green's function and C is a constant. In order to solve the above integral, we obtain the proper formula for an
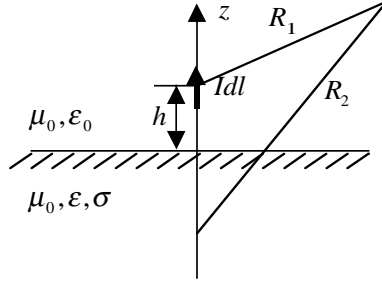
Figure 2. Vertical electric element above half-space.

electrical current element and then change the Green's function to a simple form.

3. CURRENT ELEMENT

A z-directed vertical electrical current element with length dl and at a height h, above the ground surface is shown in Fig. 2.

Based on Sommerfeld presentation, the vector and scalar Green's functions for this source, respectively are as follow [5]:

$$G_A^{zz} = \frac{\mu_0}{4\pi} \left[\frac{e^{-jk_0 r_0}}{r_0} + \frac{n^2 - 1}{n^2 + 1} \frac{e^{-jk_0 r_0'}}{r_0'} + \frac{2n^2}{n^2 + 1} U \right] \tag{2}$$

and

$$G_q = \frac{1}{4\pi\varepsilon_0} \left[\frac{e^{-jk_0 r_0}}{r_0} + \frac{n^2 - 1}{n^2 + 1} \frac{e^{-jk_0 r_0'}}{r_0'} - \frac{2n^2}{n^2 + 1} U \right] \tag{3}$$

with U as the Sommerfeld integral term. The z-component of the radiation electric field is obtained as:

$$E_z = \frac{Idl}{j4\pi\omega\varepsilon_0} \left[\frac{\partial^2}{\partial z^2} + k_0^2 \right] \left[g_0(z, z') + \frac{n^2 - 1}{n^2 + 1} g_1(z, z') + \frac{2n^2}{n^2 + 1} U \right] \tag{4}$$

where I is current distribution and $g_0(z, z')$ denotes the free space Green function, i.e.,

$$g_0(z, z') = \frac{e^{-jk_0 R_1}}{R_1} \tag{5}$$

While $g_1(z, z')$ follows from image theory:

$$g_1(z, z') = \frac{e^{-jk_0 R_2}}{R_2} \tag{6}$$

in which k_0 and k_1 are the propagation constants of free space and lossy ground, respectively, and R_1 and R_2 are the distances from the antenna and from its image to the observation point. The medium of lower half-space is taken to be lossy ground characterized by $(n^2 \varepsilon_0, \mu_0)$, with $n^2 = k_1^2/k_0^2 = \varepsilon_r - j\sigma/\omega\varepsilon_0$, where ε_r is the relative dielectric constant, and σ is the conductivity of the medium.

The first two terms in Eq. (1) determine the dipole radiation over a perfectly conducting half-space. The fact that the ground is an imperfectly conducting medium is taken into account by means of correction terms in the form of Sommerfeld integral. This integral drives from Sommerfeld problem for infinitesimal current source radiating above a lossy half-space [5]. The Sommerfeld integral U is defined as:

$$U = k_0 \int_0^\infty \frac{1}{u_0} \frac{u_0 - u_1}{n^2 u_0 + u_1} e^{-k_0 u_0 (z+h)} J_0(k_0 \lambda \rho) \lambda d\lambda \tag{7}$$

Where $u_0 = \sqrt{\lambda^2 - 1}$, $u_1 = \sqrt{\lambda^2 - n^2}$, $\rho = [(x - x')^2 + (y - y')^2]^{\frac{1}{2}}$, and $J_0(k_0 \lambda \rho)$ is the zero-order Bessel function, while h is the distance from the interface to the antenna.

3.1. Complex Image Formulation

The integrand in the Sommerfeld integral, U, is a weakly damped quasi-oscillatory complex function, which greatly complicates accurate numerical evaluation of the integral and makes it quite lengthy [5]. By applying the Discrete Complex Image Method (DCIM) [6, 7] method and Generalized Pencil Of Function (GPOF) [8, 9] technique, the $(u_0 - u_1)/(n^2 u_0 + u_1)$ term in U can be approximated by

$$\frac{u_0 - u_1}{n^2 u_0 + u_1} = \sum_{i=1}^N a_i e^{b_i u_0} \tag{8}$$

Therefore, using Sommerfeld equality, U is transformed to

$$U = \sum_{i=1}^N a_i \frac{e^{-jk_0 r_i}}{r_i} \tag{9}$$
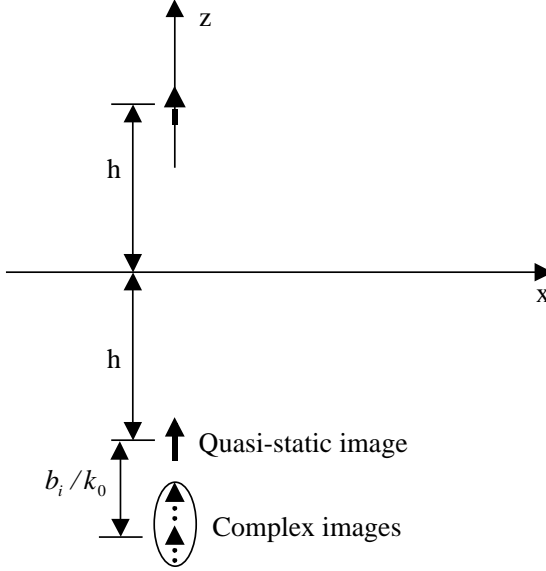
**Figure 3.** Complex images of current element above lossy ground.

where

$$r_i = \sqrt{\rho^2 + \left(z + h - \frac{b_i}{k_0}\right)^2}, \quad z \geq 0$$

The physical picture of Eq. (9) is clear. It represents N complex images located at the complex locations $(x', y', -h + b_i/k_0)(i = 1, 2, \ldots, N)$, as shown in Fig. 3.

3.2. Complex Coefficients

The coefficients, a_i, b_i, are obtained by using a nonlinear approximation scheme to put a complex function of the real argument into exponential functions. There are several techniques for this transformation, such as Prony method, modified Prony, and GPOF techniques. Prony is a noise sensitive method and therefore it has a lower accuracy. In this paper we use GPOF to obtain the complex coefficients. To use these methods, it is necessary to find an approximation path, along which the complex argument u_0 is linearly related to the real argument. Therefore the following variable change is done [6].

$$u_0 = t + j\left(1 - \frac{t}{T_0}\right) \qquad t \in [0, T_0] \tag{10}$$
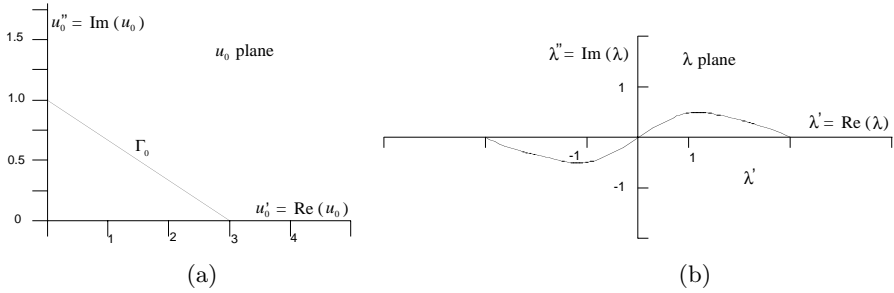
Figure 4. Approximate paths in u_0 and λ planes.

if we define $f(t)$ function as

$$f(t) = \sum_{i=1}^{N} A_i e^{S_i t} \qquad t \in [0, T_0] \tag{11}$$

then we can obtain the complex coefficients

$$
\begin{aligned}
a_i &= A_i \exp\left(-\frac{j s_i}{1 - j/T_0}\right) \\
b_i &= \frac{s_i}{1 - j/T_0}
\end{aligned}
\tag{12}
$$

where, s_i, A_i can be obtained from Eq. (11) using the GPOF method.

3.3. Selection of T_0 and N

T_0 is the truncation point of definition process of complex images. The approximate paths will be changed according to different T_0 parameter. These approximate paths in u_0 and λ planes are shown in Fig. 4(a) and Fig. 4(b). The error value occurred from different paths isn't similar to each other. The error values in spectral domain may cause high error in space domain for far zone fields. Therefore for defining the value of T_0 for far region, it is necessary to consider it with high attention. By repeatition and recursive iterations, we can achieve the suitable value of T_0.

Number of exponential terms or complex images is denoted with N. For achieving more accuracy, the value of N may be increased. For an acceptable accuracy, $N = 5$ is enough.

4. THE EQUIVALENT IMAGES FOR CURRENT SOURCES (VED, VMD, HED, AND HMD)

Based on the above mentioned discrete complex image theory, the equivalent images of short dipole can be determined considering the relevant Green's function. The results of vertical and horizontal dipoles are as follows:

4.1. Vertical Electric Dipole (VED)

Assume a z directed current distribution, i.e.,

$$\vec{J} = J_z \hat{a}_z \tag{13}$$

The equivalent discrete complex images will result in the form of

$$\vec{I_0} = \frac{n^2 - 1}{n^2 + 1} J_z \hat{a}_z \qquad \text{at} \quad z = -h \tag{14}$$

and

$$\vec{I_i} = \frac{2n^2}{n^2 + 1} a_i J_z \hat{a}_z \quad \text{at} \quad z = -h + \frac{b_i}{k_0} \quad i = 1, 2, \ldots, N \tag{15}$$

where a_i and b_i are complex coefficients obtained from DCIT.

4.2. Horizontal Electric Dipole (HED)

In this case, the current distribution is assumed as

$$\vec{J} = J_x \hat{a}_x \tag{16}$$

which yields the Green's potentials as

$$G_A^{xx} = \frac{\mu_0}{4\pi} \left[\frac{e^{-jk_0 r_0}}{r_0} + V \right] \tag{17}$$

and

$$G_q = \frac{1}{4\pi\varepsilon_0} \left[\frac{e^{-jk_0 r_0}}{r_0} - \frac{n^2 - 1}{n^2 + 1} \frac{e^{-jk_0 r_0'}}{r_0'} + \frac{2}{n^2 + 1} U \right] \tag{18}$$

and the equivalent discrete images are denoted by

$$\vec{I_i} = a_i' J_x \hat{a}_x \qquad z = -h + \frac{b_i'}{k_0} \qquad i = 1, 2, \ldots, N \tag{19}$$

where a_i' and b_i' are the complex coefficients and V is defined as

$$V = k_0 \int_0^\infty \frac{1}{u_0} \frac{u_0 - u_1}{u_0 + u_1} e^{-k_0 u_0 (Z+h)} J_0(k_0 \lambda \rho) \lambda d\lambda \tag{20}$$

4.3. Vertical Magnetic Dipole (VMD)

The magnetic current source is assumed as

$$\vec{M} = M_z \hat{a}_z \tag{21}$$

and the corresponding Green's potentials are derived as

$$G_{Am}^{zz} = \frac{\varepsilon_0}{4\pi} \left[\frac{e^{-jk_0 r_0}}{r_0} + V \right] \tag{22}$$

and

$$G_{qm} = \frac{1}{4\pi\mu_0} \left[\frac{e^{-jk_0 r_0}}{r_0} - V \right] \tag{23}$$

the discrete complex images will therefore be reduced to:

$$\vec{I_i} = a_i' M_z \hat{a}_z \qquad \text{at} \quad z = -h + \frac{b_i'}{k_0} \tag{24}$$

4.4. Horizontal Magnetic Dipole (HMD)

We assume the corresponding distribution as

$$\vec{M} = M_x \hat{a}_x \tag{25}$$

in which the Green's potentials are derived as

$$G_{Am}^{xx} = \frac{\varepsilon_0}{4\pi} \left[\frac{e^{-jk_0 r_0}}{r_0} + \frac{n^2 - 1}{n^2 + 1} \frac{e^{-jk_0 r_0'}}{r_0'} + \frac{2n^2}{n^2 + 1} U \right] \tag{26}$$

and

$$G_{qm} = \frac{1}{4\pi\mu_0} \left[\frac{e^{-jk_0 r_0}}{r_0} + 2U - V \right] \tag{27}$$

the complex images are determined as

$$\vec{I_0} = \frac{n^2 - 1}{n^2 + 1} M_x \hat{a}_x \qquad \text{at} \quad z = -h \tag{28}$$

and

$$\vec{I_i} = \frac{2n^2}{n^2 + 1} a_i M_x \hat{a}_x \qquad \text{at} \quad z = -h + \frac{b_i}{k_0} \quad i = 1, 2, \dots, N \tag{29}$$

5. CURRENT DISTRIBUTION ON THE APERTURE ANTENNA

The current distribution on the aperture surface is considered as a continuous array of short dipole elements which are continuously located across the aperture.

Applying the above mentioned nonclassical image theory which was introduced for dipole and wire antennas in previous articles [1–3], known as discrete complex image theory (DCIT), the complex images of the mentioned dipole elements can be determined.

Considering the linear behavior of the subject and the possibility of using the superposition principle, the obtained images are in fact in the form of some planes appeared in the complex locations. Fig. 5 shows the sketch of these images.
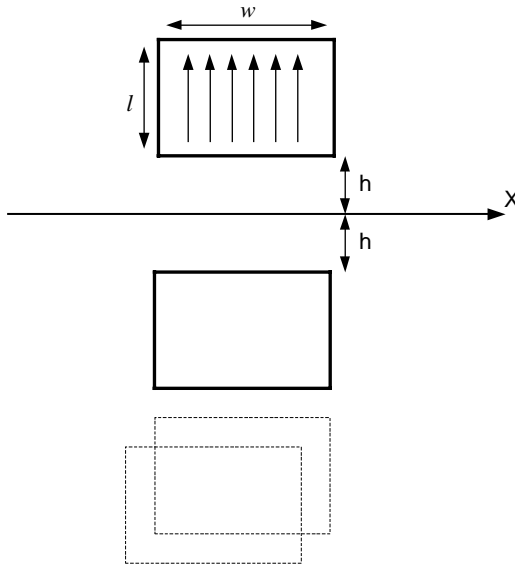
Figure 5. Sketch of complex image planes.

We denote the tangential components of the aperture fields by $\vec{E}_a$ and $\vec{H}_a$. The equivalent current sources according to the equivalence principle are achieved as follow

$$\vec{J} = \hat{n} \times \vec{H}_a \tag{30}$$

and

$$\vec{M} = -\hat{n} \times \vec{E}_a \tag{31}$$

Using the proposed method to evaluating the complex images of this current distribution, the fields of aperture antennas can be determined.

As an example; consider a uniform aperture distribution:

$$\vec{E}_a = E_0 \hat{a}_x \tag{32}$$

and

$$\vec{H}_a = H_0 \hat{a}_z \tag{33}$$

The complex image sources associated with this current distribution are obtained as:

$$I_i = a'_i J_x = a'_i H_0 \quad i=1,2,\ldots,N \quad -h+\frac{b'_i}{k_0}-\frac{w}{2} \le z \le -h+\frac{b'_i}{k_0}+\frac{w}{2}$$

and
$$\tag{34}$$

$$I_{mi} = a'_i M_z = a'_i E_0 \qquad -\frac{l}{2} \le x \le \frac{l}{2}$$

As the program is running in first time these complex images will be determined in a short time.

6. RADIATION FIELDS

Considering the complex images and the original source, they construct a linear array. Based on the principle of pattern multiplication and using the similarity property of the array elements the resultant array factor can be defined as

$$E_{total} = E_{Element} \cdot AF \tag{35}$$

the aperture fields formulas have been introduced in text books. Array factor for our geometry can be determined as:

$$AF = \sum_{i=1}^{N+1} I_n e^{jk_0 z_n \cos\theta} = e^{jk_0(h+\frac{l}{2})\cos\theta} + \sum_{i=1}^{N} a'_i e^{-jk_0(h+\frac{l}{2}-\frac{b'_i}{k_0})\cos\theta}$$
$$\tag{36}$$

where, I_n is the relative current for each element, z_n corresponds to the center of each element, and N is number of elements. The far region fields can be calculated easily by

$$E_\theta = -jk_0 e^{-jk_0 r}(L_\phi + \eta N_\theta)/(4\pi r)$$
$$E_\phi = jk_0 e^{-jk_0 r}(L_\theta - \eta N_\phi)/(4\pi r) \tag{37}$$
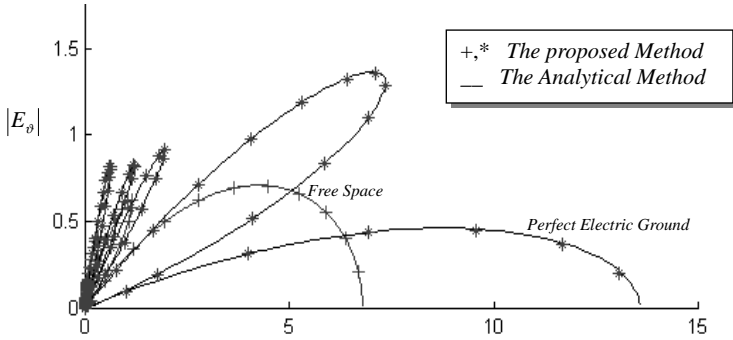
Figure 6. Comparison of results for the perfect electric ground and free space.

6.1. Numerical Results

As the first example, we consider the uniform current distribution on the aperture. We assume the field distribution as

$$\vec{H}_a = H_0\hat{a}_x \qquad -\frac{w}{2} \le x' \le \frac{w}{2} \qquad -\frac{l}{2} \le z' \le \frac{l}{2} \qquad (38)$$

Therefore the equivalent current on the surface of aperture will be obtained as follows:

$$\vec{J} = H_0\hat{a}_z \tag{39}$$

the array factor of the equivalent array will then be obtained as

$$AF = e^{jk_0(h+\frac{l}{2})\cos\theta} + \frac{n^2-1}{n^2+1}e^{-jk_0(h+\frac{l}{2})\cos\theta} + \sum_{n=1}^{N}\frac{2n^2}{n^2+1}e^{-jk_0\left[(h+\frac{l}{2})-\frac{b_i}{k_0}\right]\cos\theta} \tag{40}$$

Using Eqs. (35) and (37), the radiation fields of the aperture will be obtained. To verify the validity of the proposed approach we consider the limiting cases. For perfect electric ground ($\sigma \to \infty$) and for free space ($n = 1$), we calculate the radiation field and compare it to the analytical results. Fig. 6 shows such a comparison.

Consider a lossy ground with $\varepsilon_r = 10$ and $\sigma = 10\,\mathrm{mS/m}$. We calculate the radiation field, E_θ, for the aperture above earth. Fig. 7 shows the obtained results.

This figure illustrates the effect of finite conductivity on the pattern. It affects the angle of mainlobe, SLL and sidelobes. The
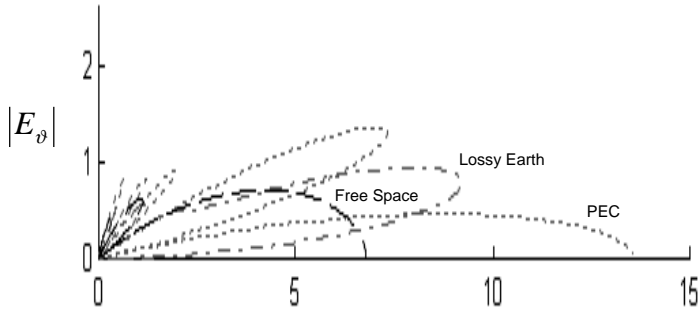
Figure 7. Radiation pattern of aperture with $l = 3\lambda$, $w = 2\lambda$, and the height $h = \lambda$ above a perfect electric conductor and lossy ground with $\varepsilon_r = 10$, and $\sigma = 10\,\text{mS/m}$.

Table 1. Relative permittivity and conductivity for water and earth.

	ε_r	$\sigma, s/m$
Sea Water	80	1
Fresh Water	80	10^{-3}
Wet Earth	20	10^{-2}
Dry Earth (Sand)	4	10^{-3}

mainlobe angle changes from 90 degrees to 85 degrees and the first sidelobe reduce from $-5.2\,\text{dB}$ to $-17.3\,\text{dB}$.

To illustrate the effect of lossy earths, we consider the real earths which their parameters listed in Table 1.

Fig. 8 shows the effect of real earths on the pattern of aperture antennas. It is observed that the gain, mainlobe and sidelobes of radiation patterns is affected by the conduction coefficients and dielectric constants.

The second example is an aperture with a tapered distribution. Consider a cosine distribution over the aperture as follow
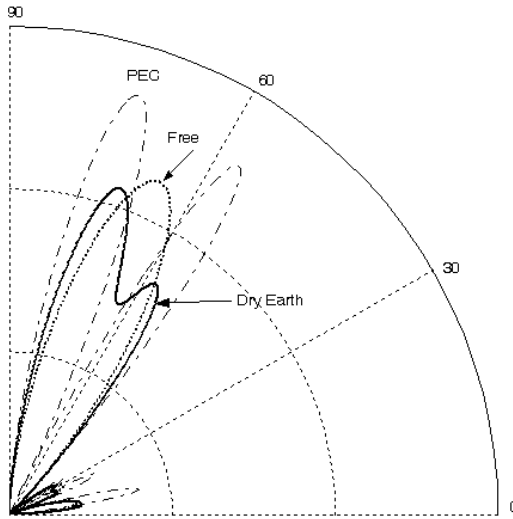
$$\vec{E} = a_z E_0 \cos\left(\frac{\pi}{w}x'\right) \qquad -\frac{w}{2} \leq x' \leq \frac{w}{2} \qquad -\frac{l}{2} \leq z' \leq \frac{l}{2} \quad (41)$$

The equivalent current on the surface of aperture is therefore, a horizontal magnetic current as

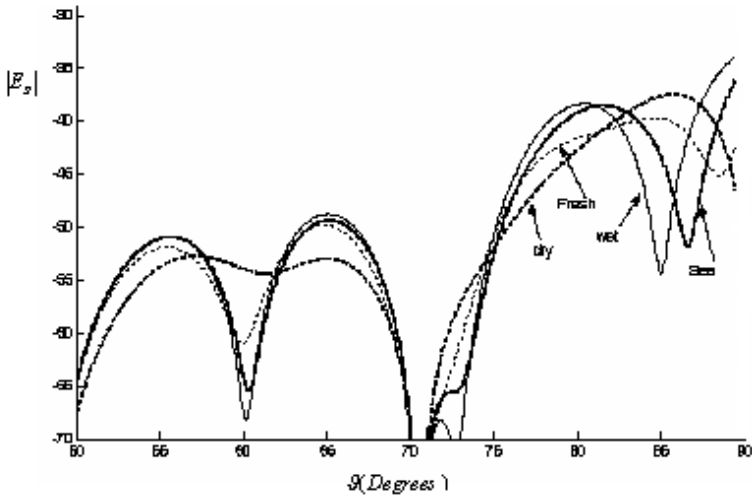$$\vec{M} = \hat{a}_x E_0 \cos\left(\frac{\pi}{w}x'\right) \quad (42)$$
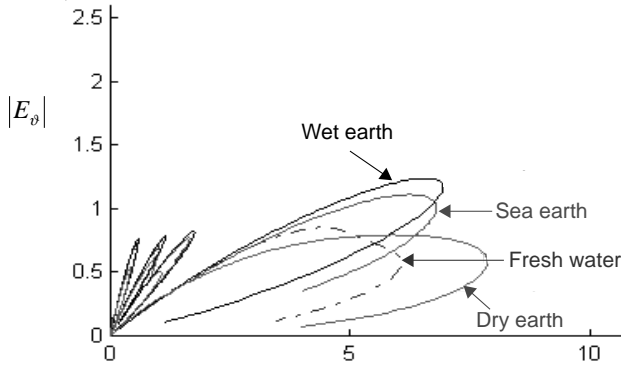
Figure 8. Radiation pattern of aperture antennas of Fig. 7 located above real earths of Table 1.

Figure 9. Radiation patterns of apertures of Fig. 7 located above dry earth, PEC, and free space.

Based on the duality and Eqs. (28) and (29), the array factor is similar to the Eq. (40) and the radiation fields can be obtained from the Eqs. (35) and (37). As a result, we compare the radiation pattern of the aperture with the above mentioned distribution while located above perfect electric conductor, dry earth and in free space. Fig. 9 shows this radiation patterns in the $\phi = 0$ plane.

Figure 10. The radiation patterns of aperture of Fig. 7 located above real earths of Table 1.

As is observed, tapered distribution cause to reduce the sidelobes similar to PEC and free space. The effect of finite conductivity of an imperfect earth can be illustrated for the entries of Table 1. Fig. 10 shows the obtained radiation pattern in $\phi = 90$ degrees plane.

We can select any electric or magnetic distribution on the surface of aperture and apply the proposed approach. The present problem assumes infinite, flat, and homogeneous lossy half-space with parameters ε_r and σ. Comparison of the resulted image with those obtained from Sommerfeld integral formulation shows that for $h > 0.01\lambda$ the differences are negligible. The method is applicable for all bands and can be used for high or low frequencies. The important feature of the image method is in less computational time and better convergence.

7. CONCLUSION

The proposed complex image method for analyzing aperture antennas yields satisfactory results and accuracy. This method conceptually is very simple and less time consuming because the complex images will be computed in a very shorter time than the Sommerfeld integrals. Using this method in analyzing aperture antennas above real ground is a new and interested achievement. Contrary to other image methods,

for each pair of ε_r and σ, we have to find a specific set of complex images independent of source or field point locations. Since the complex-image coefficients are independent of the spatial co-ordinates, numerical integration of the Sommerfeld integrals for the entire field and source locations are not needed. The numerical implementation is easily performed on a personal computer.

Although, due to the complexity of Sommerfeld integrals, a simple method for the analysis of aperture antennas above ground is not reported, the proposed DCIM with proper number of images is practically accurate for aperture antennas. The radiation pattern of this type antennas and scatterers above or below real or multilayer ground can be obtained with a little additional computation compared to the free space radiation.

ACKNOWLEDGMENT

REFERENCES

1. Abbasi, B. and M. Hakkak, "Analysis of electromagnetic radiation with an electric dipole above lossy ground using complex image theory," *ICT2002 Conference,* Vol. 3, Beijing, June 2002.

2. Abbasi, B. and M. Hakkak, "Analysis of vertical electric dipole above lossy half-space using discrete complex image method," *IEEE APS/URSI Symposium,* AT&M Texas University, June 2002.

3. Hakkak, M. and B. Abbasi, "Analysis of vertical wire antenna above imperfect ground using discrete complex image method," *MMET 02 Conference,* Ukraine, Sept. 2002.

4. Popovic, B. D. and V. V. Petrovic, "Vertical wire antenna above ground: Simple near exact Image solution," *IEE Proceedings-H,* Vol. 140, No. 6, 501–507, Dec. 1993.

5. Banos, A., *Dipole Radiation in the Presence of a Conducting HalfSpace,* Pergamon, New York, 1966.

6. Fang, D. G., J. J. Yang, and G. Y. Delisle, "Discrete image theory for horizontal electric dipoles in multilayered medium," *IEE Proc.-H,* Vol. 135, No. 5, 297–303, 1988.

7. Chow, Y. L., et al., "A closed form spatial Green's function for the thick microstrip substrate," *IEEE, Trans. Microwave Theory Technique,* Vol. 39, No. 3, 588–592, 1991.

8. Sarkar, T. K. and O. Pereira, "Using the matrix pencil method to estimate the parameters of a sum of complex exponentials," *IEEE AP Magazine,* Vol. 37, No. 1, 48–55, Feb. 1995.

9. Hue, Y. and T. K. Sarkar, "Generalized pencil-offunction method for extracting poles of an EM system from its transient response," *IEEE Trans. Antennas Propagat.,* Vol. 37, 229–234, Feb. 1989.